iScience

CellPress

Article

Mosquito Midgut Prostaglandin Release Establishes Systemic Immune Priming

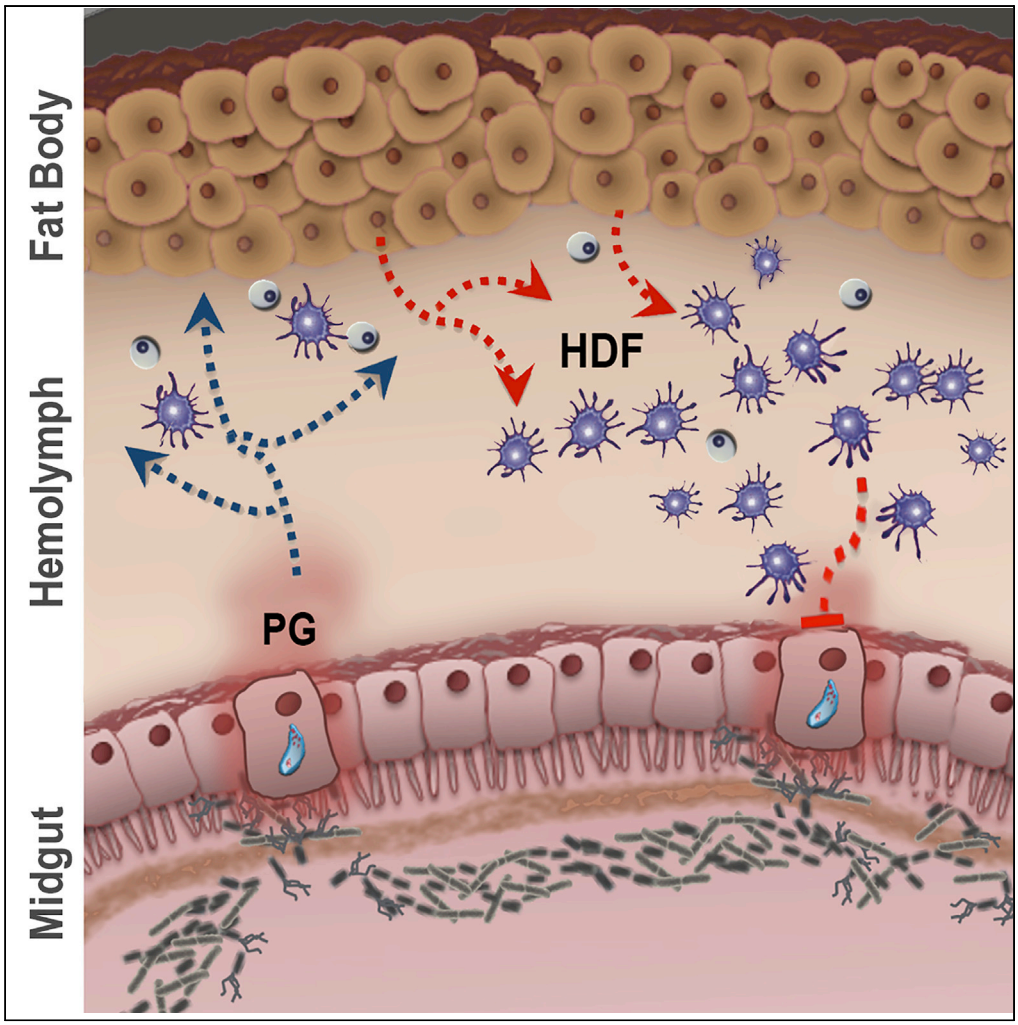

Ana Beatriz F. Barletta, Nathanie Trisnadi, Jose Luis Ramirez, Carolina Barillas-Mury

cbarillas@niaid.nih.gov

HIGHLIGHTS

Plasmodium invasion or bacterial exposure triggers midgut prostaglandin synthesis

Prostaglandins attract mosquito hemocytes and increase their patrolling activity

Two midgut peroxidases, HPX7 and HPX8, catalyze midgut prostaglandin synthesis

Systemic release of midgut prostaglandins is essential to establish immune priming

Barletta et al., iScience *19*, 54–62
September 27, 2019
https://doi.org/10.1016/j.isci.2019.07.012

iScience

CellPress

Article

Mosquito Midgut Prostaglandin Release Establishes Systemic Immune Priming

Ana Beatriz F. Barletta,[1] Nathanie Trisnadi,[1,3] Jose Luis Ramirez,[1,2] and Carolina Barillas-Mury[1,4,*]

SUMMARY

***Anopheles gambiae* mosquitoes that have been infected with *Plasmodium* mount a more effective immune response to a subsequent infection. Priming is established when *Plasmodium* invasion of the mosquito midgut allows contact of the gut microbiota with epithelial cells. This event is followed by a systemic release of a hemocyte differentiation factor (HDF) consisting of Lipoxin A4 bound to Evokin, a lipocalin carrier, which increases the proportion of circulating hemocytes. We show that mosquito midgut cells produce and release prostaglandin E2 (PGE2), which attracts hemocytes to the midgut surface and enhances their patrolling activity. Systemic injection of prostaglandins (PGs) recapitulates the priming response and enhances antiplasmodial immunity by triggering HDF production. Although insects lack cyclooxygenases, two heme peroxidases, HPX7 and HPX8, catalyze essential steps in PG biosynthesis in mosquitoes. Mosquito midgut PGE2 release attracts hemocytes and establishes a long-lasting enhanced systemic cellular immune response to Plasmodium infection.**

INTRODUCTION

Anopheles gambiae mosquitoes can mount an effective antiplasmodial immune response that involves the coordinated activation of epithelial (Oliveira Gde et al., 2012), cellular (Castillo et al., 2017) and complement-like immune defenses (Blandin et al., 2004; Povelones et al., 2009; Fraiture et al., 2009). *Plasmodium* ookinete midgut invasion triggers immune priming by bringing the gut microbiota into direct contact with midgut cells (Rodrigues et al., 2010). Primed mosquitoes release a hemocyte differentiation factor (HDF) into their hemolymph and mount a more effective immune response to subsequent *Plasmodium* infections (Rodrigues et al., 2010). HDF release is a life-long response and results in a permanent increase in the proportion of circulating granulocytes and a state of enhanced immunity (Rodrigues et al., 2010). HDF is a complex of Lipoxin A4, a signaling eicosanoid, and Evokin, a lipid carrier of the lipocalin protein family that is essential for biological activity (Ramirez et al., 2015). Although the interaction of bacteria with epithelial cells takes place in the midgut lumen, the priming response is systemic and sustained, suggesting that the midgut epithelium releases a signal that elicits broad changes in immune function. In this study, we provide direct experimental evidence for the role of prostaglandin E2 (PGE2) as a chemotactic signal that attracts hemocytes to the basal surface of *An. gambiae* midgut cells and as the midgut signaling molecule that establishes immune priming. Furthermore, we identified two mosquito heme peroxidases that mediate midgut PGE2 synthesis and are essential for hemocyte chemotaxis and immune priming.

RESULTS AND DISCUSSION

Effect of *Plasmodium* Infection and Bacterial Exposure on Prostaglandin Synthesis and Systemic Release

PGE2 has been detected in cultured *Anopheles albimanus* mosquito midguts in the presence of gut bacteria (Garcia Gil de Muñoz et al., 2008), and several studies have shown that blood feeding leads to bacterial proliferation in the mosquito midgut (Dong et al., 2009). Therefore, we investigated the potential role of prostaglandins (PGs) on mosquito responses to blood feeding and *Plasmodium* infection. We observed a significant increase in mosquito hemolymph PG levels at 24 h post blood feeding (PF) on a healthy control mouse (Figure 1A, $p = 0.0062$, *Unpaired t test*, Table S1). In uninfected mosquitoes, the gut microbiota is kept from coming in direct contact with the midgut epithelium by the peritrophic matrix (PM), a chitinous network that surrounds the blood meal. Ookinete midgut invasion disrupts the PM, allowing direct contact between bacteria and midgut epithelial cells. PG levels were 6-fold higher in females fed on a *P. berghei*-infected mouse than those fed on a healthy mouse at 24 h PF, when ookinete midgut invasion is taking place (Figure 1A, $p < 0.0001$, *Unpaired t test*, Table S1). We investigated the role of the gut microbiota on *Plasmodium*-induced production of PG and confirmed that, in the presence of the gut microbiota,

[1]Laboratory of Malaria and Vector Research, National Institute of Allergy and Infectious Diseases, National Institutes of Health, Rockville, MD 20852, USA

[2]Present address: Crop Bioprotection Research Unit, Agricultural Research Service, U.S. Department of Agriculture, Peoria, IL 61604, USA

[3]Present address: Atropos Therapeutics Inc., San Carlos CA 94070, USA

[4]Lead Contact

*Correspondence: cbarillas@niaid.nih.gov

https://doi.org/10.1016/j.isci.2019.07.012

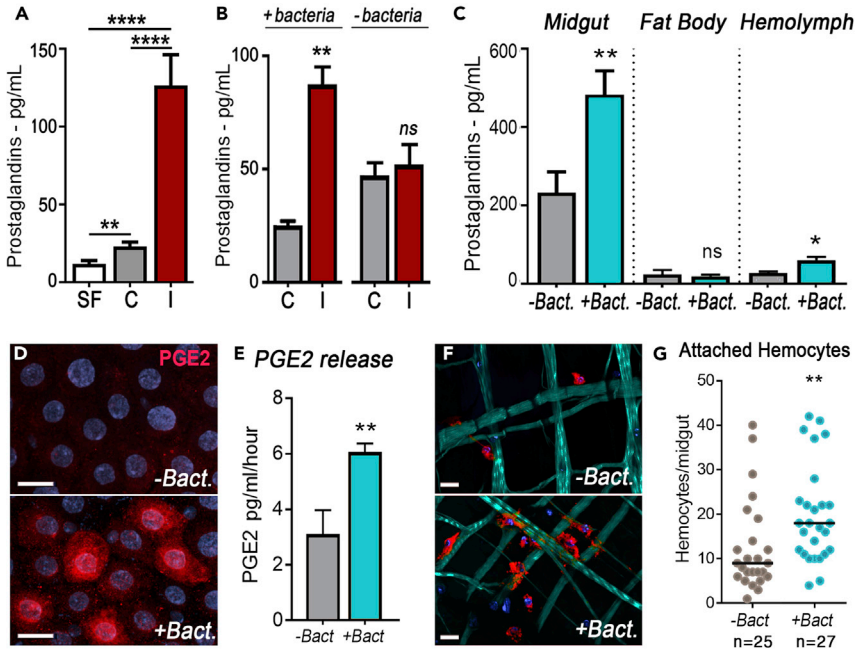

Figure 1. Effect of *Plasmodium* Infection and Bacterial Exposure on Prostaglandin Synthesis and Systemic Release

(A) Hemolymph prostaglandin levels in sugar fed (SF), blood-fed control (C), and *P. berghei* infected (I).

(B) Hemolymph prostaglandin levels in response to gut microbiota in blood-fed control (C) and *P. berghei*-infected (I) mosquitoes 26 h post infection.

(C) Prostaglandin levels in different tissues 24 h after bacterial feeding.

(D) PGE2 midgut immunostaining 6 h after bacterial feeding. Nuclei, blue; PGE2, red. Scale bar: 10 μm.

(E) *In vitro* PGE2 release by midguts dissected 6 h after bacterial feeding.

(F) Hemocytes recruitment to the basal surface of the midgut in response to bacterial feeding. Actin (phalloidin), cyan; Hemocytes (stained with Vybrant CM-DiI), red; Nuclei, blue. Scale bar: 15 μm.

(G) Number of hemocytes attached to the midgut 6 h post bacterial feeding.

Error bars in A–C and E represent mean ± SEM. ANOVA Tukey's multiple comparison test was used in A. Unpaired t test was used in B, C, and E. *$p \leq 0.05$; **$p \leq 0.01$; ****$p \leq 0.0001$; NS, $p > 0.05$. Prostaglandin levels were measured in pools of hemolymph. Each treatment had at least two biological replicates, and the results were confirmed in at least two independent experiments. In G, hemocyte numbers were determined for each individual midgut and the median are indicated by the line. Hemocytes were counted in 5–12 mosquitoes for each treatment, and the results were confirmed in three independent experiments. Mann-Whitney test, **$p \leq 0.01$. Detailed information on biological replicates and exact p values are listed in Tables S1–S5.

ookinete invasion increased PG release (Figures 1A and 1B, $p = 0.0043$, *Unpaired t test*, Tables S1 and S2). However, this effect was no longer observed when the gut microbiota was eliminated by pre-treating mosquitoes with oral antibiotics (Figure 1B, $p = 0.6943$, *Unpaired t test*, Table S2).

We investigated the production of PGs by different tissues in response to bacterial feeding. Adult females were fed a sterile BSA solution supplemented with arachidonic acid (BSA + AA), an essential precursor in PG synthesis normally present in vertebrate blood, and dissected 24 hours after feeding. PG levels were low in the fat body and hemolymph, close to the lowest limit of detection of the ELISA assay. In contrast, PG levels were about 10-fold higher and clearly detectable in the midgut (Figure 1C). Midgut PG levels increased by 2-fold when live bacteria were included in the BSA + AA solution (Figure 1C, $p = 0.0042$, *Unpaired t test*, Table S3), accompanied by a modest but significant increase in the hemolymph (Figure 1C, $p = 0.0376$, *Unpaired t test*, Table S3). However, the presence of bacteria had no effect on PG levels in the fat body (Figure 1C, $p = 0.5705$, *Unpaired t test*, Table S3). The absence of PG in the bacteria + BSA + AA suspension was confirmed, ruling it out as the source of PG (Figure S1). PGE2 immunofluorescence staining 6 h post-feeding was strong in the midguts of females fed bacteria (Figure 1D). Some cells stained stronger than others, and overall, PGE2 staining was most prominent in the perinuclear region (Figure 1D). Furthermore, when midguts of females fed sterile or bacteria-containing BSA were dissected and

cultured *in vitro*, the rate of PGE2 secretion was significantly higher in the presence of bacteria (Figure 1E, p = 0.0079, *Unpaired t test*, Table S4). While investigating the effect of ingestion of bacteria on the interaction of hemocytes with the mosquito midgut, we observed that phagocytosed bacteria in hemocytes were associated with the midgut basal lamina in females that received BSA with bacteria (Figure S2). Additionally, a significant increase in the number of hemocytes attached to the basal surface of the midgut was observed 6 h after females were fed a BSA-bacterial suspension (Figures 1F and 1G, p = 0.0028, *Mann-Whitney U test*, Table S5), suggesting that PG release by the midgut attracts hemocytes.

Effect of PGE2 on Mosquito Hemocyte Chemotaxis and Patrolling Activity

We tested this hypothesis *in vitro* by placing *An. gambiae* hemocyte-like Sua 5.1 cells in a culture dish with an agarose spot containing either PGE2 or a buffer control. Cells were allowed to settle for 4 h, and their movements were followed in real time (Figure 2A and Videos S1 and S2). After 12 h, an average of 25 cells/field migrated under the agarose spots containing PGE2, whereas no migration was observed under the control spots (Figure 2B, p < 0.0001, *Mann-Whitney U test*, Table S6). In similar experiments with PGF2, significant chemotaxis was also observed (Figure S3, p = 0.0104, *Mann-Whitney U test*, Table S7), but the rate of migration was significantly lower than with PGE2 (6.8 cells/field; p < 0.0001, *Mann-Whitney U test*, Table S6). The effect of bacterial feeding on hemocyte dynamics was evaluated by imaging midgut-associated hemocytes in live females fed on sterile BSA or BSA containing bacteria. Hemocytes were labeled by systemic injection of a lipophilic dye (Vybrant CM-DiD) and imaged for 2 h, starting at 4 h post-feeding. Only hemocytes that remained associated with the midgut surface for at least 1 hour were included in the analysis. Midgut-associated hemocytes from females fed BSA with bacteria traveled a longer distance and moved faster than those from females fed sterile BSA (Figure 2C, Videos S3 and S4). The distance traveled (track length) during the first hour of observation was significantly longer (Figure 2D, p < 0.0001, *Mann-Whitney U test*, Table S8), and the speed (total distance/total time of observation) was significantly higher (Figure 2E, p < 0.0001, *Mann-Whitney U test*, Table S9) in females that ingested BSA containing bacteria. The positive chemotactic response of hemocytes to PGE2 released by the midgut when cells come in direct contact with bacteria could limit potential systemic bacterial infections, and would be particularly important when ookinetes traverse the PM and disrupt the midgut epithelium.

Effect of Bacterial Immune Elicitors on Prostaglandin Synthesis and Immune Priming

Direct contact between bacteria and midgut cells is necessary to establish immune priming (Rodrigues et al., 2010), suggesting that midgut PG release might be involved in this response. Therefore, we investigated whether systemic injection of PGs previously detected in insects (PGE1, PGE2, and PGF2) (Garcia Gil de Muñoz et al., 2008, Stanley-Samuelson and Ogg, 1994; Ramos et al., 2014) could recapitulate the priming response. Injection of PGE1, PGE2, or PGF2 significantly increased the proportion of circulating granulocytes (Figure 3A, p = 0.0015, <0.0001, and <0.0001, respectively, *Mann-Whitney U test*, Table S10), with PGE2 having the strongest effect. Systemic injection of PGE2 also enhanced antiplasmodial immunity, significantly reducing the number of oocysts (Figure 3B, p = 0.0016, *Mann-Whitney U test*, Table S11), whereas the effects of PGE1 and PGF2 on *Plasmodium* infection were not statistically significant (Figure 3B, p = 0.1842 and p = 0.0582, respectively, *Mann-Whitney U test*, Table S11).

We further investigated the effects of PG injections by exploring the hypothesis that they trigger long-lasting HDF activity in hemolymph. As expected, owing to the short half-life of PGs (Samuelsson et al., 1975), hemolymph collected 4 days after female mosquitoes were injected with PGs contained low levels of PGs that were not significantly different from those of control mosquitoes injected with buffer (Figure S4, p = 0.7693, *ANOVA Dunn's multiple comparison test*, Table S12). Transfer of this hemolymph from females pre-treated with PGE1 or PGE2 into naive females increased the proportion of granulocytes relative to untreated controls (Figure 3C, p = 0.0025 and p < 0.0001, respectively, *Mann-Whitney U test*, Table S13). PGE2 elicited the strongest response, whereas PGF2 pre-treatment had no effect (Figure 3C, p = 0.6075, *Mann-Whitney U test*, Table S13). Furthermore, silencing Evokin, the carrier protein component of HDF in the donor, before PGE2 injection, eliminated the effect of this eicosanoid on hemocyte differentiation in recipient mosquitoes (Figure 3D, *dsLacZ*, p = 0.0015 and *dsEvokin*, p = 0.5101, *Mann-Whitney U test*, Table S14). Taken together, these observations indicate that PGE2 injection triggers long-lasting HDF release into the mosquito hemolymph, prompting the immune priming response.

Next, we investigated whether increased contact with immune elicitors from the endogenous gut flora was sufficient to induce priming. The diffusion of bacteria-derived immune elicitors out of the mosquito midgut

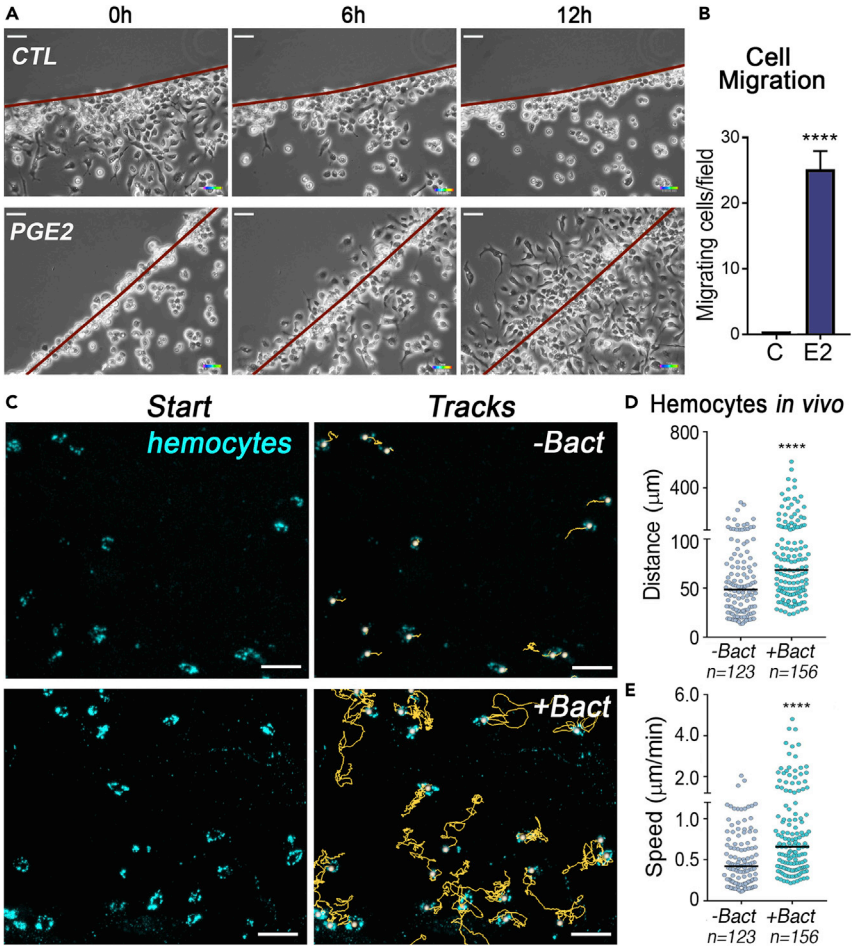

Figure 2. Effect of PGE2 on Mosquito Hemocyte Chemotaxis and Patrolling Activity

(A) Time-lapse imaging of Sua5.1 hemocyte-like cells migrating in an agarose spot assay in response to PBS (CTL) or 7 µg of PGE2 (PGE2). Scale bar: 30 µm.

(B and C) (B) Quantification of motile cells per field in the PBS control (C) and PGE2 (E2) agarose spots. Error bars in (B) represent mean ± SEM. Unpaired t test, ****$p \leq 0.0001$. Quantification of cell migration was performed in at least two independent experiments with two biological replicates for each treatment. Detailed information on biological replicates and exact p values are listed in Table S6 (see Videos S1 and S2). (C) Snapshot of live mosquito hemocytes (cyan) in their initial position. The yellow lines represent hemocyte movement tracked for a minimum of 1 h.

(D) Hemocyte distance traveled in 1 h. Each dot represents the distance traveled by individual hemocytes during the first hour of video imaging.

(E) Hemocyte speed. Each dot represents the mean speed of individual hemocytes during the whole duration of the video imaging. Medians are indicated by the lines. Four midguts were analyzed for each condition and a total of 123 hemocytes in the -Bact and 156 hemocytes in the +Bact. Mann-Whitney test, ****$p \leq 0.0001$. Scale bar: 20 µm. Detailed information on biological replicates and exact p values are listed in Tables S8 and S9 (see Videos S3 and S4).

lumen is tightly regulated by an Immunomodulatory Peroxidase (IMPer) (Kumar et al., 2010). IMPer is secreted into the ectoperitrophic space, between the PM and the midgut epithelium, and cross-links the proteins present in this space (Kumar et al., 2010). IMPer silencing increases the permeability of the ectoperitrophic space, allowing soluble immune elicitors to interact with the midgut epithelium (Kumar et al., 2010). Silencing IMPer significantly enhanced PG levels in the hemolymph 24 h after ingestion of a blood meal (Figure 3E, $p = 0.0001$, *Unpaired t test*, Table S15), a time when the gut microbiota undergoes extensive proliferation. Reducing IMPer expression also significantly increased the number of hemocytes associated with basal surface of the midgut (Figures 3F and 3G, $p = 0.0005$, *Mann-Whitney U test*, Table S16) and increased the proportion of circulating granulocytes (Figure 3H, $p < 0.0001$, *Mann-Whitney U test*, Table S17). Furthermore, transfer of hemolymph collected 4 days after blood feeding from IMPer-silenced

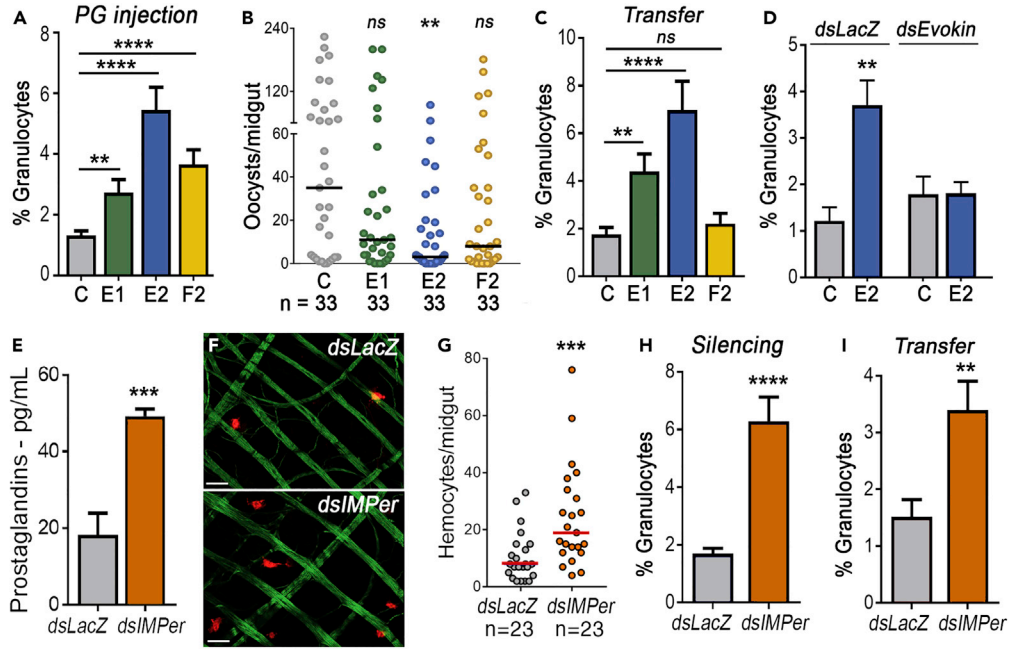

Figure 3. Effect of Bacterial Immune Elicitors on Prostaglandin Synthesis and Immune Priming

(A) Effect of systemic prostaglandin injection on the proportion of circulating granulocytes.

(B) Mosquito susceptibility to *P. berghei* infection after systemic injection of different prostaglandins (PGE1, PGE2, and PGF2).

(C) Effect of hemolymph transfer from mosquito donors shown in (A), collected 4 days after PG injection, on the proportion of circulating granulocytes in the recipients.

(D) Effect of Evokin silencing on the biological activity of hemolymph of females transferred 4 days after PGE2 injection, measured as the effect on the proportion of circulating hemocytes in the recipients.

(E) Effect of IMPer silencing on hemolymph prostaglandin levels 48 h post blood feeding.

(F and G) Effect of IMPer silencing on the number of hemocytes attached to the midgut basal surface 12 h after blood feeding. Actin (phalloidin), cyan; Hemocytes (stained with Vybrant CM-DiI), red. Scale bar: 15 μm.

(H) Effect of IMPer silencing on the proportion of circulating granulocytes after blood feeding.

(I) Effect of hemolymph transfer from IMPer-silenced donor, collected 4 days after blood feeding, on the proportion of circulating hemocytes in the recipients.

Error bars in A, C–E, H, and I represent mean ± SEM. Mann- Whitney U test and Unpaired t test, **$p \leq 0.01$; ***$p \leq 0.001$; ****$p \leq 0.0001$. Hemocyte counting in C, D, H, and I were obtained from at least 5–10 individual mosquitoes for each treatment in at least two independent experiments. Each dot in B and G represent the number of oocysts or hemocytes, respectively, for individual midguts. The median is indicated by the line. Mann-Whitney U test, **$p \leq 0.01$; ***$p \leq 0.001$, NS, $p > 0.05$. Detailed information on biological replicates and exact p values are listed in Tables S10, S11, and S13–S18.

mosquitoes to naive recipients also increased the proportion of granulocytes (Figure 3I, $p = 0.003$, *Mann-Whitney U test*, Table S18).

Role of Two Midgut Peroxidases on Prostaglandin Synthesis and Immune Priming

Although PGs have been detected in insects, whole-genome sequencing of multiple species indicates that they lack an ortholog of vertebrate cyclooxygenase (Varvas et al., 2009), suggesting that PG synthesis is mediated by some other enzyme(s) (Garcia Gil de Muñoz et al., 2008, Stanley-Samuelson and Ogg, 1994; Chotiwan et al., 2018). We confirmed our previous observation (Kumar et al., 2010) that feeding mosquito with a BSA solution containing bacteria induces expression of two heme peroxidases, HPX7 and HPX8 (Figure S5, $p = 0.0003$ and $= 0.0002$, respectively, Mann-Whitney U test, Table S19). IMPer silencing also induces the expression of these two enzymes 24 h PF (Figure 4A, $p = 0.0022$ and $p = 0.004$, respectively, *Mann- Whitney U test*, Table S20). Furthermore, co-silencing IMPer and HPX7 (Figure 4B, $p = 0.7701$, *ANOVA* Dunn's *multiple comparison*, Table S21) or IMPer and HPX8 (Figure 4C, $p = 0.8520$, *ANOVA* Dunn's *multiple comparison*, Table S22) prevents the increase in PG release after blood feeding that is observed when IMPer alone is silenced (Figure 4B, $p = 0.0003$ and 4C $p = 0.0002$, ANOVA Dunn's multiple comparison, Tables S21 and S22). Similarly, the increase in hemocyte binding to the basal surface of the midgut in

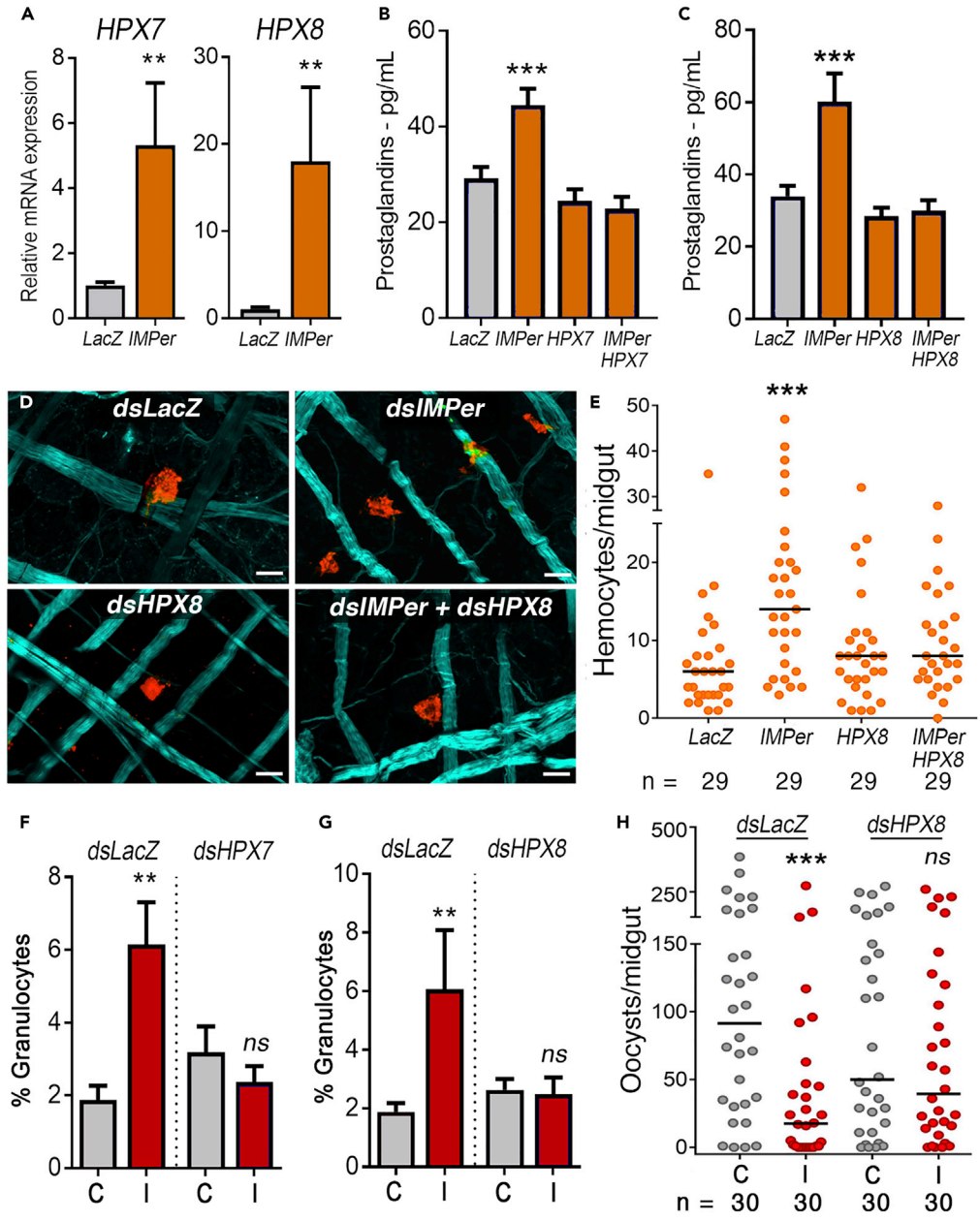

Figure 4. Role of Two Midgut Peroxidases on Prostaglandin Synthesis and Immune priming

(A) Relative mRNA expression of HPX7 and HPX8 in the midgut, 48 h post blood-meal, in LacZ (control) and IMPer-silenced mosquitoes.

(B) Effect of IMPer and HPX7 co-silencing on hemolymph prostaglandin levels 48 h after blood feeding.

(C) Effect of IMPer and HPX8 co-silencing on hemolymph prostaglandin levels 48 h after blood feeding.

(D and E) Effect of IMPer, HPX8, or IMPer + HPX8 co-silencing on the number of hemocytes attached to the basal surface of the midgut 12 h post blood feeding. Actin (phalloidin), cyan; Hemocytes (stained with Vybrant CM-DiI), red. Scale bar: 15 μm.

(F) Effect of hemolymph transfer from LacZ controls and HPX7-silenced donors, collected 4 days after feeding on a control (C) or a *P.berghei* infected (I) mouse, on the proportion of circulating hemocytes in the recipients.

(G) Effect of hemolymph transfer from LacZ controls and HPX8-silenced donors, collected 4 days after feeding on a control (C) or a *P.berghei*-infected (I) mouse, on the proportion of circulating hemocytes in the recipients.

(H) Effect of hemolymph transfer from LacZ controls and HPX8-silenced donors on the antiplasmodial immunity of the recipients. Hemolymph was collected 4 days post-feeding on control (C) or a *P.berghei*-infected (I) mouse.

Figure 4. *Continued*

Error bars in A–C, F, and G represent mean ± SEM. Mann-Whitney U test and Unpaired t test, **$p \leq 0.01$; ***$p \leq 0.001$, NS, $p > 0.05$. In A–C, 2–3 pools per treatment were used in at least two independent experiments. In F and G, granulocyte numbers were counted in at least 5–10 individual mosquitoes. Each dot in E and H represent the number of hemocytes or oocysts, respectively, for each individual midgut. The median is indicated by the line. Detailed information on biological replicates and exact p values are listed in Tables S20–S26.

IMPer-silenced females (Figures 4D and 4E, p = 0.0005, *ANOVA Kruskal-Wallis test*, Table S23) is no longer observed when HPX8 is co-silenced with IMPer (Figures 4D and 4E, p = 0.1289, *ANOVA Kruskal-Wallis test*, Table S23).

We also evaluated the potential participation of these two heme peroxidases in mosquito immune priming after *P. berghei* infection. When either HPX7 (Figure 4F, p = 0.0022, *Mann-Whitney U test*, Table S24) or HPX8 (Figure 4G, p = 0.0036, *Mann-Whitney U test*, Table S25) was silenced, the increase in the proportion of granulocytes after infection (a hallmark of immune priming) was no longer observed (Figures 4F and 4G, p = 0.3930 and p = 0.5795, respectively, *Mann-Whitney U test*, Tables S24 and S25). Furthermore, exposure of HPX8-silenced females to *Plasmodium* infection no longer enhanced antiplasmodial immunity when their hemolymph was transferred to naive mosquitoes (Figure 4H, p = 0.0009 and p = 0.5154, *Mann-Whitney U test*, Table S26), in agreement with the lack of HDF activity in the donors (Figure 4G).

Disruption of the peroxidase *pxt* gene in *Drosophila* resulted in sterile female flies, but follicle maturation was rescued *in vitro* by treatment with PG (Tootle and Spradling, 2008) and fertility was restored *in vivo* by expressing the mammalian COX-1 protein (Tootle and Spradling, 2008). This study suggests that PGs are necessary for *Drosophila* follicle maturation and that vertebrate COX1 can complement the biological function of *pxt* by restoring PG synthesis. However, direct evidence of PG synthesis by *pxt* was not provided. Our findings agree with these observations and indicate that, besides their role in development, PGs also participate in antimicrobial responses. Additional studies indicate that indomethacin inhibits vertebrate thyroid peroxidase and lactoperoxidase (Van Zyl and Louw, 1979) in addition to cyclooxygenase, suggesting that peroxidases may be the targets of this drug in insects. This could explain the pharmacological effect of indomethacin on antibacterial response in lepidoptera (Downer et al., 1997) and *Plasmodium* sporozoite infection in mosquitoes (Ramos et al., 2014). Furthermore, there are reports that vertebrate peroxidases can catalyze PG synthesis *in vitro* using arachidonic acid as a substrate (Zilletti et al., 1989; Panganamala et al., 1974; Egan et al., 1979). Our findings suggest that HPX7 and HPX8 assume the role of cyclooxygenase in converting arachidonic acid to intermediate endoperoxides, such as PGH2, whereas the Prostaglandin E enzymes that convert PGH2 to PGE2 are conserved.

PGs differ in their biological activity in mosquitoes. Although injection of PGE1, PGE2, and PGF2 all increased the proportion of circulating granulocytes, PGE2 elicited the strongest response and significantly enhanced antiplasmodial immunity. Although both PGE1 and PGF2 also reduced *Plasmodium* infection, their effect was more modest and did not reach statistical significance. PGE2 also evoked a stronger chemotactic response from hemocyte-like cells (Sua 5.1 cell line) than did PGF2. Furthermore, synthesis of PGE2 by midgut cells in mosquitoes fed a BSA solution containing bacteria was documented using a PGE2-specific monoclonal antibody. Taken together, our results indicate that *An. gambiae* mosquitoes can synthesize PGE2 and that this PG has the strongest biological activity. The precise mechanism by which HPX7 and HPX8 are involved in PGE2 synthesis remains to be established.

Based on our findings, we propose the following mechanism for the establishment of mosquito immune priming in response to *Plasmodium* infection. When ookinetes invade the midgut, bacteria come in contact with epithelial cells and induce expression of HPX7 and HPX8. The induction of these two enzymes mediates PGE2 synthesis by midgut epithelial cells. PG release, in turn, attracts hemocytes, enhances their patrolling activity, and establishes immune priming. The initial PGE2 release by midgut epithelial cells has long-lasting effects on the mosquito immune system and is a key signal for the establishment of a life-long state of enhanced immunity. In vertebrates, lipopolysaccarides (LPS) has been shown to stimulate PGE2 synthesis and release by alveolar epithelial cells (Speth et al., 2016). PGE2, in turn, modulates local inflammation by triggering secretion of SOCS3-containing microparticles by alveolar macrophages. We conclude that the release of PGE2 by epithelial cells is an ancient innate immunomodulatory response that is conserved from insects to vertebrates.

Limitations of the Study

Although we observe that midgut PG attracts hemocytes, we do not have specific markers available to determine which hemocyte type is being recruited. RNA knockdown of HPX7 and HPX8 decreased the amount of PG in the hemolymph, but since silencing is transient and depends on the protein turnover, we were not able to altogether abolish PG production. To fully characterize the role of HPX7 and HPX8 in PG synthesis, we must develop knockout mosquitoes for those enzymes.

METHODS

All methods can be found in the accompanying Transparent Methods supplemental file.

DATA AND CODE AVAILABILITY

The raw data and detailed information on individual experiments and number of replicates are available in the Supplementary tables file.

SUPPLEMENTAL INFORMATION

Supplemental Information can be found online at https://doi.org/10.1016/j.isci.2019.07.012.

ACKNOWLEDGMENTS

This work was supported by the Intramural Research Program of the Division of Intramural Research Z01AI000947, NIAID, National Institutes of Health, and by NIH Grant P01GM095467. We thank André Laughinghouse and Kevin Lee for insectary support and Roxanne Withers for editing help. A.B.F.B. was supported by Conselho Nacional de Desenvolvimento Científico e Tecnológico (CNPq), Brazil.

AUTHOR CONTRIBUTIONS

Experiments were designed by A.B.F.B., N.T., J.L.R, and C.B.-M.; carried out by A.B.F.B., J.L.R., and N.T.; and analyzed by A.B.F.B., N.T., J.L.R, and A.B.F.B. C.B.-M. wrote the paper.

DECLARATION OF INTERESTS

The authors declare no competing financial interests.

Received: January 23, 2019
Revised: May 10, 2019
Accepted: July 8, 2019
Published: September 27, 2019

REFERENCES

Blandin, S., Shiao, S.H., Moita, L.F., Janse, C.J., Waters, A.P., Kafatos, F.C., and Levashina, E.A. (2004). Complement-like protein TEP1 is a determinant of vectorial capacity in the malaria vector *Anopheles gambiae*. Cell *116*, 661–670.

Castillo, J.C., Ferreira, A.B.B., Trisnadi, N., and Barillas-Mury, C. (2017). Activation of mosquito complement antiplasmodial response requires cellular immunity. Sci. Immunol. *2*, eaal1505.

Chotiwan, N., Andre, B.G., Sanchez-Vargas, I., Islam, M.N., Grabowski, J.M., Hopf-Jannasch, A., Gough, E., Nakayasu, E., Blair, C.D., Belisle, J.T., et al. (2018). Dynamic remodeling of lipids coincides with dengue virus replication in the midgut of *Aedes aegypti* mosquitoes. PLoS Pathog. *14*, e1006853.

Dong, Y., Manfredini, F., and Dimopoulos, G. (2009). Implication of the mosquito midgut microbiota in the defense against malaria parasites. PLoS Pathog. *5*, e1000423.

Downer, R.G., Moore, S.J., L Diehl-Jones, W., and Mandato, C.A. (1997). The effects of eicosanoid biosynthesis inhibitors on prophenoloxidase activation, phagocytosis and cell spreading in *Galleria mellonella*. J. Insect Physiol. *43*, 1–8.

Egan, R.W., Gale, P.H., and Kuehl, F.A., Jr. (1979). Reduction of hydroperoxides in the prostaglandin biosynthetic pathway by a microsomal peroxidase. J. Biol. Chem. *254*, 3295–3302.

Fraiture, M., Baxter, R.H., Steinert, S., Chelliah, Y., Frolet, C., Quispe-Tintaya, W., Hoffmann, J.A., Blandin, S.A., and Levashina, E.A. (2009). Two mosquito LRR proteins function as complement control factors in the TEP1-mediated killing of *Plasmodium*. Cell Host Microbe *5*, 273–284.

Garcia Gil de Muñoz, F.L., Martinez-Barnetche, J., Lanz-Mendoza, H., Rodriguez, M.H., and Hernandez-Hernandez, F.C. (2008). Prostaglandin E2 modulates the expression of antimicrobial peptides in the fat body and midgut of *Anopheles albimanus*. Arch. Insect Biochem. Physiol. *68*, 14–25.

Kumar, S., Molina-Cruz, A., Gupta, L., Rodrigues, J., and Barillas-Mury, C. (2010). A peroxidase/dual oxidase system modulates midgut epithelial immunity in *Anopheles gambiae*. Science *327*, 1644–1648.

Oliveira Gde, A., Lieberman, J., and Barillas-Mury, C. (2012). Epithelial nitration by a peroxidase/NOX5 system mediates mosquito antiplasmodial immunity. Science *335*, 856–859.

Zilletti, L., Ciuffi, M., Moneti, G., Franchi-Micheli, S., Valoti, M., and Sgaragli, G.P. (1989). Peroxidase catalysed formation of prostaglandins from arachidonic acid. Biochem. Pharmacol. *38*, 2429–2439.

Panganamala, R.V., Sharma, H.M., Sprecher, H., Geer, J.C., and Cornwell, D.G. (1974). A suggested role for hydrogen peroxide in the

biosynthesis of prostaglandins. Prostaglandins *8*, 3–11.

Povelones, M., Waterhouse, R.M., Kafatos, F.C., and Christophides, G.K. (2009). Leucine-rich repeat protein complex activates mosquito complement in defense against *Plasmodium* parasites. Science *324*, 258–261.

Ramirez, J.L., de Almeida Oliveira, G., Calvo, E., Dalli, J., Colas, R.A., Serhan, C.N., Ribeiro, J.M., and Barillas-Mury, C. (2015). A mosquito lipoxin/lipocalin complex mediates innate immune priming in *Anopheles gambiae*. Nat. Commun. *6*, 7403.

Ramos, S., Custodio, A., and Silveira, H. (2014). *Anopheles gambiae* eicosanoids modulate *Plasmodium* berghei survival from oocyst to salivary gland invasion. Mem. Inst. Oswaldo Cruz. *109*, 668–671.

Rodrigues, J., Brayner, F.A., Alves, L.C., Dixit, R., and Barillas-Mury, C. (2010). Hemocyte differentiation mediates innate immune memory in *Anopheles gambiae* mosquitoes. Science *329*, 1353–1355.

Samuelsson, B., Granstrom, E., Green, K., Hamberg, M., and Hammarstrom, S. (1975). Prostaglandins. Annu. Rev. Biochem. *44*, 669–695.

Speth, J.M., Bourdonnay, E., Penke, L.R., Mancuso, P., Moore, B.B., Weinberg, J.B., and Peters-Golden, M. (2016). Alveolar epithelial cell-derived prostaglandin E2 serves as a request signal for macrophage secretion of suppressor of cytokine signaling 3 during innate inflammation. J. Immunol. *196*, 5112–5120.

Stanley-Samuelson, D.W., and Ogg, C.L. (1994). Prostaglandin biosynthesis by fat body from the tobacco hornworm, *Manduca sexta*. Insect Biochem. Mol. Biol. *24*, 481–491.

Tootle, T.L., and Spradling, A.C. (2008). Drosophila Pxt: a cyclooxygenase-like facilitator of follicle maturation. Development *135*, 839–847.

Varvas, K., Kurg, R., Hansen, K., Jarving, R., Jarving, I., Valmsen, K., Lohelaid, H., and Samel, N. (2009). Direct evidence of the cyclooxygenase pathway of prostaglandin synthesis in arthropods: genetic and biochemical characterization of two crustacean cyclooxygenases. Insect Biochem. Mol. Biol. *39*, 851–860.

Van Zyl, A., and Louw, A. (1979). Inhibition of peroxidase activity by some non-steroidal anti-inflammatory drugs. Biochem. Pharmacol. *28*, 2753–2759.

ISCI, Volume *19*

Supplemental Information

Mosquito Midgut Prostaglandin Release Establishes Systemic Immune Priming

Ana Beatriz F. Barletta, Nathanie Trisnadi, Jose Luis Ramirez, and Carolina Barillas-Mury

Supplemental Information

Mosquito midgut prostaglandin release establishes systemic immune priming

Ana Beatriz Ferreira Barletta[1], Nathanie Trisnadi[1], Jose Luis Ramirez[1, 2], Carolina Barillas-Mury[1*, #].

[1]Laboratory of Malaria and Vector Research, National Institute of Allergy and Infectious Diseases, National Institutes of Health, Rockville, MD 20852, United States.

[2]Present address: Crop Bioprotection Research Unit, Agricultural Research Service, U.S. Department of Agriculture, Peoria, IL 61604, United States.

*** Correspondent author: cbarillas@niaid.nih.gov (CB-M)**

[#] Lead author: cbarillas@niaid.nih.gov (CB-M)

Supplemental Figures

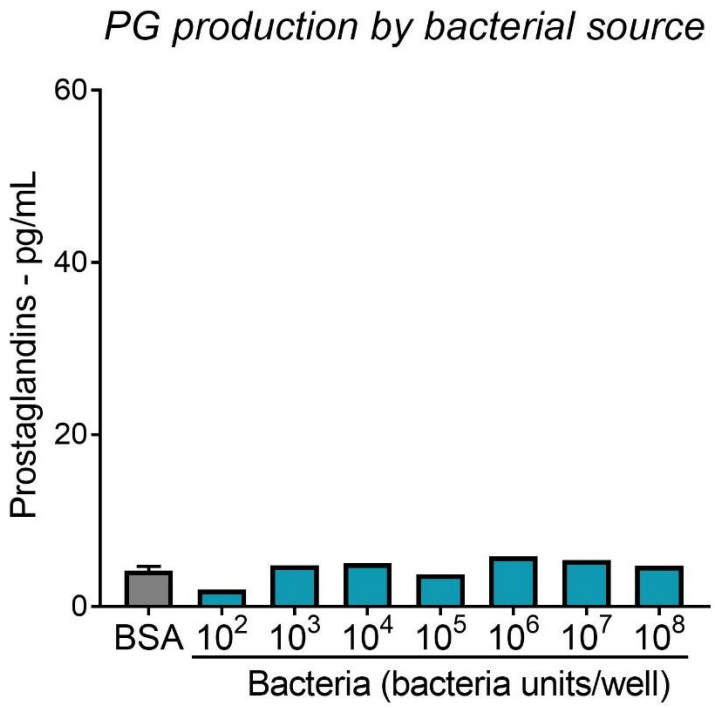

Figure S1. PG production by bacterial source, related to Figure 1. Prostaglandin levels were measured by ELISA in a BSA suspension containing crescent amounts of bacteria, ranging from 100 to 100.000.000 bacteria/ well. Levels were calculated in pg/mL and compared with BSA solution without bacteria.

\

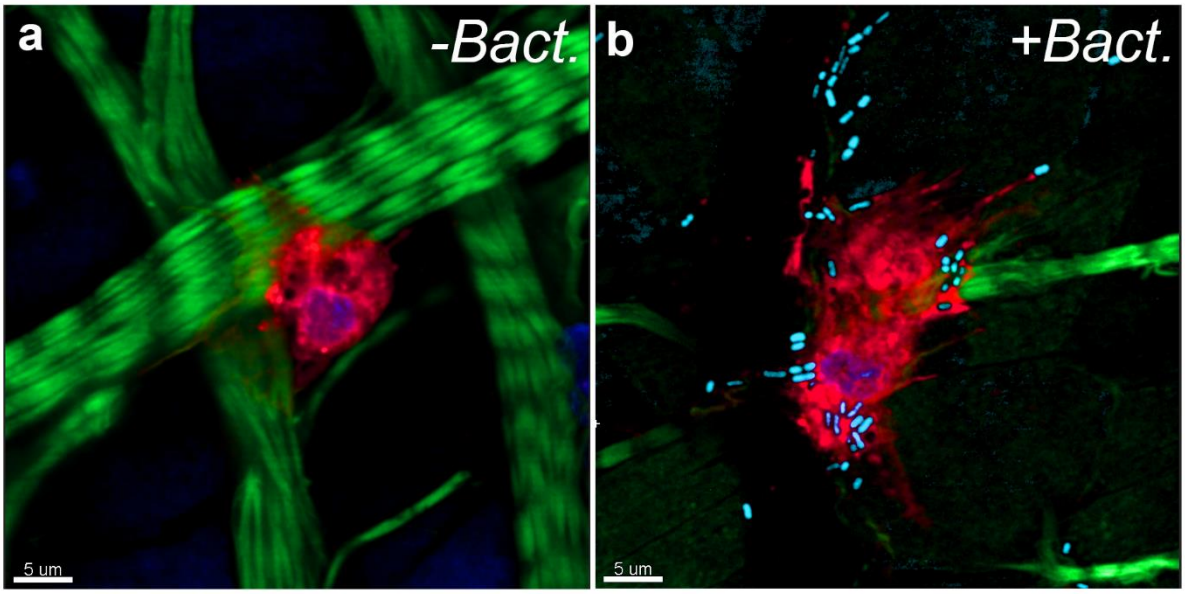

Figure S2. Intracellular bacteria can be observed in hemocytes associated with midgut basal surface, related to Figure 1. (a) Hemocyte attached to the midgut basal surface in control mosquitoes fed with BSA 6 hours post feeding. **(b)** Hemocyte attached to the midgut basal surface in mosquitoes fed with bacteria 6 hours post feeding. Bacteria is observed inside and in close contact with hemocytes attached to basal lamina. Actin, green; Hemocytes, red; Nuclei, blue; Bacteria, cyan. Scale bar: 5μm.

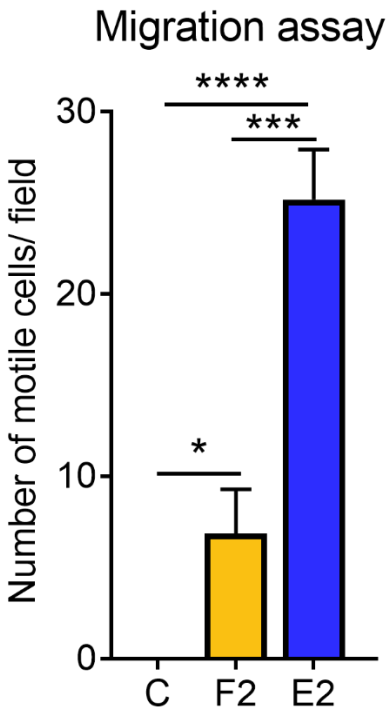

Figure S3. PGF2 chemotaxis, related to Figure 2. Quantification of motile Sua 5.1 *Anopheles* cells per field after exposure to PBS (Ctr) and 7 μg of PGF2 and PGE2 for 16 hours. Error bars represent mean ± SEM. ANOVA Dunn's multiple comparison test, *P≤0.05, ***P≤0.001, ****P≤0.0001. Quantification of migrating cells was performed in at least 2 independent experiments. In each experiment 10 fields per treatment were randomly chosen and counted. Detailed information of biological replicates and exact p values are listed in supplementary table 6 and 7.

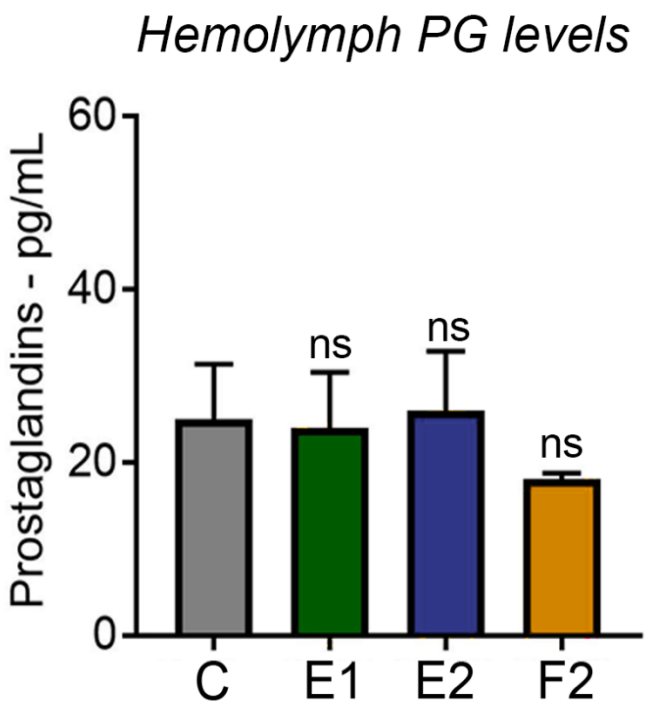

Figure S4. PG measurement on the hemolymph of PG treated mosquitoes 4 days post injection, related to Figure 3. Hemolymph prostaglandin levels four days after prostaglandin systemic injection. Mosquitoes were injected with 500nM of PGE1 (E1), PGE2 (E2) or PGF2 (F2). Error bars represent mean ± SEM. *ANOVA* Dunn's multiple comparison, NS, P>0.05. Each experimental group was compared with the control. The hemolymph of 10 mosquitoes was polled per biological replicate. At least 2 independent experiments were performed. Detailed information of biological replicates and exact p value number are listed in supplementary table 12.

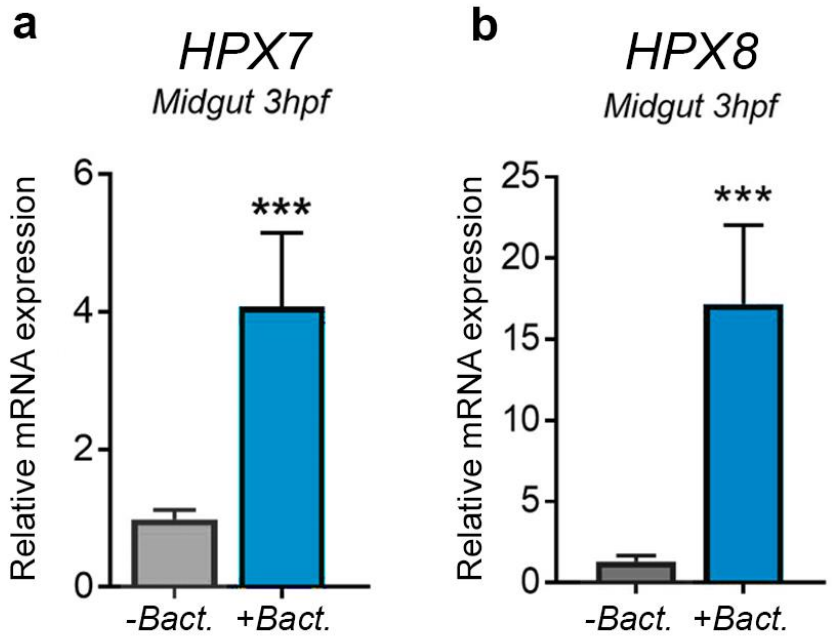

Figure S5. Gene expression of HPX7 and HPX8 in the midgut 3 hours after bacterial feeding, related to Figure 4. (a) HPX7 relative mRNA expression in the midgut 3 hours post feeding (3hpf) with BSA (-Bact) or BSA containing bacteria (+Bact). Error bars in **a** and **b** represent mean ± SEM. Mann-Whitney U test, ***P≤0.001. Fifteen midguts were pooled for each biological replicate. Two independent experiments with at least 2 biological replicates for each treatment. Detailed information of biological replicates and exact p value number are listed in supplementary table 19.

Video S1. Sua 5.1 migration activity in response to PBS. Related to Figure 2.

Video S2. Sua 5.1 migration activity in response to PGE2 exposure. Related to Figure 2.

Video S3. Hemocyte patrolling activity in control mosquitoes. Related to Figure 2.

Video S4. Hemocyte patrolling activity in bacteria fed mosquitoes. Related to Figure 2.

Supplementary tables

Groups	Exp 1	Exp 2	Exp 3	Comparison	P value
Sugar fed (SF)	20.37 ± 1.53, n=4	7.87 ± 0.424, n=4	5.743 ± 0.6664, n=3	SF Vs C	0.7193
Blood fed (C)	19.8 ± 2.224, n=4	24.3 ± 3.136, n=4	26.93 ± 14.43, n=2	C Vs I	< 0.0001
P.berghei INF (I)	127.3 ± 53.65, n=2	113.7 ± 39.42, n=4	142.7 ± 19.21, n=3	SF Vs I	< 0.0001

Table S1 – Prostaglandin levels in the hemolymph in response to *P.berghei* infection 24 hours post feeding. Related to Figure 1. (SF) sugar fed. (C) Blood fed control. (I) *P.berghei* infected. *ANOVA Tukey's multiple comparison test*. **Each n is a biological replicate of a pool of 10 mosquitoes. Each independent experiment has at least 2 biological replicates (2 pools of 10 mosquitoes).**

Groups	Exp 1	Exp 2	Comparison	P value
Blood fed (C) + bacteria	24.99 ± 3.642, n=3	25.6 ± 1.823, n=3	C +Bact Vs I+Bact	0.0043
P.berghei INF (I) + bacteria	85.94 ± 10.75, n=3	89.54 ± 11.86, n=2		
Blood fed (C) + bacteria	35.22 ± 2.463, n=4	59.28 ± 4.619, n=4	C -Bact Vs I-Bact	0.6943
P.berghei INF (I) - bacteria	59.13 ± 12.24, n=4	42.78 ± 13.42, n=3		

Table S2 – Prostaglandin levels in the hemolymph in response to *P.berghei* infection 24 hours post feeding with (+ Bact) and without (-Bact) the presence of the microbiota. Related to Figure 1. (C) Blood Fed control. (I) *P.berghei* infected. Mann-Whitney U test. **Each n is a biological replicate of a pool of 10 mosquitoes. Each independent experiment has at least 2 biological replicates (2 pools of 10 mosquitoes).**

Treatment	Group	Exp 1	Exp 2	Comparison	P value
- Bact	Midgut	211.5 ± 11.72, n=3	264.3 ± 59.33, n=2	Midgut Control Vs Bacteria	0.0042
	Fat Body	28.71 ± 10.18, n=2	19.79 ± 7.551, n=2		
	Hemolymph	28.37 ± 2.472, n=2	-	Fat Body Control Vs Bacteria	0.5705
+Bact	Midgut	443.7 ± 102.8, n=2	521.7 ± 94.17, n=2		
	Fat Body	18.51 ± 2.601, n=2	22.88 ± 0.000, n=1	Hemolymph Control Vs Bacteria	0.0376
	Hemolymph	60.95 ± 6.018, n=2	-		

Table S3 – Prostaglandin production by different tissues in response to bacterial feeding. Midgut, Fat Body and hemolymph from BSA fed (-Bact) and BSA + Bacteria fed (+Bact). Related to Figure 1. Unpaired t-test. **Each n is a biological replicate of a pool of 10 mosquito's tissues and hemolymph. Each independent experiment has at least 2 biological replicates (2 pools of 10 mosquitoes).**

Tissue	Group	Exp 1	Exp 2	Comparison	P value
Midgut	- Bact	3.553 ± 0.4916, n=3	2.444 ± 2.444, n=2	Midgut control Vs Midgut Bacteria	0.0079
	+ Bact	6.178 ± 0.5114, n=3	5.894 ± 0.3157, n=2		

Table S4 – PGE2 release by midguts in response to bacterial feeding. Related to Figure 1. Midguts from mosquitos fed with BSA (-Bact) or BSA + Bacteria (+Bact). Unpaired t-test. **Each n is a biological replicate of a pool of 10 midguts. Each independent experiment has at least 2 biological replicates (2 pools of 10 midguts).**

Treatment	Exp 1	Exp 2	Exp 3	Comparison	P value
-Bact	7, n=5	9, n=12	9, n=8	-	-
+Bact	20, n=6	17, n=11	17, n=10	Control Vs Bacteria	0.0028

Table S5 – Hemocytes attached to midgut in response to bacterial feeding. Hemocytes were visualized and counted on the midgut surface of mosquitoes fed with BSA (-Bact) or BSA + Bacteria (+Bact). Related to Figure 1. Mann-Whitney U test. **Each n represents an individual mosquito. Each independent experiment has at least 5 biological replicates (individual midguts).**

Treatment	Migration (fields)	Comparison	P value
Control	0 ± 0, n=10	-	-
E2	25.18 ± 2.753, n=11	Control Vs E2	<0.0001

Table S6 – Migration activity of SUA 5.1 after exposure to PGE2. Related to Figure 2. Agarose spot containing PBS (Control) or PGE2 was placed in contact with SUA 5.1 cells. Mann-Whitney U test. **N represents the number of fields counted for each condition.**

Treatment	Migration (fields)	Comparison	P value
Control	0 ± 0, n=15	-	-
F2	6.85 ± 2.832, n=20	Control Vs F2	0.0104

Table S7 – Migration activity of SUA 5.1 cells after exposure to PGF2. Related to Figure 2. Agarose spot containing PBS (Control) or PGF2 was placed in contact with SUA 5.1 cells. Mann-Whitney U test. **N represents the number of fields counted for each condition.**

Treatment	Distance traveled (total number of hemocytes)	Comparison	P value
-Bact	48.69, n=123	-	-
+Bact	66.95, n=156	Control Vs Bacteria	<0.0001

Table S8 – Distance traveled by hemocytes on the first hour of movie. Related to Figure 2. Total number of hemocytes from 4 midguts per treatment, from 4 independent experiments. Mann-Whitney U test. **N represents the total number of hemocytes recorded in 4 independent experiments.**

Treatment	Speed (total number of hemocytes)	Comparison	P value
-Bact	0.4224, n=123	-	-
+Bact	0.6493, n=156	Control Vs Bacteria	<0.0001

Table S9 – Hemocytes speed. Related to Figure 2. Total number of hemocytes from 4 midguts per treatment (-Bact and +Bact), from 4 independent experiments. Mann-Whitney U test. **N represents the total number of hemocytes recorded in 4 independent experiments.**

Treatment	Exp 1	Exp 2	Comparison	P value
Buffer	1.543 ± 0.1871, n=7	1.07 ± 0.1816, n=6	-	-
E1	2.344 ± 0.6015, n=6	2.969 ± 0.3665, n=8	Buffer Vs E1	0.0015
E2	4.349 ± 0.6917, n=7	6.559 ± 1.231, n=7	Buffer Vs E2	<0.0001
F2	3.176 ± 0.6019, n=7	4.077 ± 0.7272, n=8	Buffer Vs F2	<0.0001

Table S10 – Granulocyte percentage per mosquito four days after systemic prostaglandin injection. Related to Figure 3. Mann-Whitney U test**. N represents the number of individual mosquitoes used per experiment. At least 6 individual mosquitoes were used per condition for each of the 2 independent experiments.**

Treatment	Exp 1	Exp 2	Exp 3	Comparison	P value
Buffer	11.5, n=22	39, n=32	142, n=9	-	-
E1	5, n=15	9.5, n=30	137.5, n=6	Buffer Vs E1	0.1271
E2	2, n=33	14, n=21	34, n=11	Buffer Vs E2	<0.0001
F2	1, n=20	30, n=12	59, n=11	Buffer Vs F2	0.0247

Table S11 – Effect of prostaglandin systemic injection on antiplasmodial immunity. Related to Figure 3. Median number of oocysts per midgut dissected 10 days post infection. Three independent infections were performed and pooled together for analysis**.** *ANOVA Dunnet multiple comparison*. **Table represents non-randomized data and therefore treatments have different numbers of individual mosquitoes. Buffer (total n=63); PGE1 (total n=51); PGE2 (total n=65); PGF2 (total n=43).**

Treatment	Exp 1	Exp 2	Comparison	P value
Buffer	29.29, n=1	24.68 ± 6.218, n=2	-	-
E1	34.33, n=1	23.63 ± 6.333, n=2	Buffer Vs E1	0.9980
E2	27.16, n=1	25.63 ± 6.78, n=2	Buffer Vs E2	0.9986
F2	14.18, n=1	17.88 ± 0.6347, n=2	Buffer Vs F2	0.7398

Table S12 – Prostaglandin levels in the hemolymph four days after systemic injection of prostaglandin. Related to Figure 3. **Two independent experiments were conducted, and each biological replicate corresponded to a pool of 10 mosquitoes. First experiments had one biological replicate and experiment 2 has 2 pools of 10 mosquitoes. *ANOVA* Dunn's multiple comparison test.**

Treatment	Exp 1	Exp 2	Comparison	P value
Buffer	2.001 ± 0.3575, n=5	1.575 ± 0.4388, n=6	-	-
E1	3.989 ± 1.496, n=5	4.745 ± 0.6649, n=6	Buffer Vs E1	0.0025
E2	7.632 ± 2.227, n=5	6.166 ± 0.2753, n=4	Buffer Vs E2	<0.0001
F2	2.308 ± 0.7018, n=5	2.147 ± 0.5869, n=7	Buffer Vs F2	0.6075

Table S13 – Granulocytes percentage of naive mosquitoes injected with the hemolymph from prostaglandin pre-treated mosquitoes. Related to Figure 3. **Two independent experiments were performed, each one with a different batch of hemolymph. At least 4 individual mosquitoes were counted per condition in two independent experiments. Mann-Whitney U test. All individuals were considered for statistical analysis.**

Treatment	Group	Exp 1	Comparison	P value
dsLacZ	Control	1.214 ± 0.2907, n=10	dsLacZ control Vs dsLacZ E2	0.0015
	E2	3.705 ± 0.5343, n=11		
dsEvokin	Control	1.786 ± 0.3813, n=9	dsEvokin control Vs dsEvokin E2	0.5101
	E2	1.81 ± 0.2417, n=10		

Table S14 – Granulocyte percentage of *Evokin-silenced* mosquitoes injected with prostaglandin E2. Related to Figure 3. One experiment was performed and at least 9 individual mosquitoes were analyzed per condition. Mann-Whitney U test. **All individuals were considered for statistical analyses.**

Treatment	Exp 1	Comparison	P value
dsLacZ BF	18.3 ± 3.256, n=3	-	-
dsIMPer BF	49.24 ± 1.075, n=3	dsLacZ Vs dsIMPer	0.0008

Table S15 – Prostaglandin hemolymph levels in blood-fed *IMPer-silenced* mosquitoes. Related to Figure 3. Three biological replicates, containing a pool of 10 mosquitoes each, were used for dsLacZ and dsIMPer groups. Unpaired t-test. **All individuals were considered for statistical analysis.**

Treatment	Exp 1	Exp 2	Exp 3	Comparison	P value
dsLacZ	10, n=11	4, n=7	7, n=5	-	-
dsIMPer	21, n=9	14, n=5	26, n=9	dsLacZ Vs dsIMPer	0.0005

Table S16 – Number of hemocytes associated with the midgut basal surface in blood-fed *IMPer-silenced* mosquitoes. Related to Figure 3. Three independent experiments were performed and at least 5 individual mosquitoes were counted per group in each experiment. **All individuals were considered for statistical analysis. Mann-Whitney U test.**

Treatment	Exp 1	Exp 2	Comparison	P value
dsLacZ BF	1.917 ± 0.2524, n=9	1.451 ± 0.2583, n=8	-	-
dsIMPer BF	5.443 ± 1.098, n=9	7.125 ± 1.271, n=9	dsLacZ Vs dsIMPer	<0.0001

Table S7– Granulocyte percentage in blood-fed IMPer-silenced mosquitoes. Related to Figure 3. Two independent experiments were performed and at least 8 individual mosquitoes were counted per experimental group. Mann-Whitney U test. **All individuals were considered for statistical analysis.**

Hemolymph injection from	Exp 1	Exp 2	Comparison	P value
dsLacZ BF	0.9124 ± 0.2232, n=10	2.387 ± 0.5136, n=7	-	-
dsIMPer BF	2.554 ± 0.2817, n=10	4.09 ± 0.8691, n=12	dsLacZ Vs dsIMPer	0.0030

Table S18 – Granulocyte percentage in naïve mosquitoes injected with the hemolymph of blood-fed *IMPer-silenced* mosquitoes. Related to Figure 3. Two independent experiments were performed with different batches of hemolymph. At least 7 individual mosquitoes were counted in each experimental group. Mann-Whitney U test. **All individuals were considered for statistical analysis.**

Gene	Treatment	Exp 1	Exp 2	Exp 3	Comparison	P value
HPX7	-Bact	1.235 ± 0.4633, n=3	1.007 ± 0.08537, n=3	1.053 ± 0.3286, n=2	-	-
	+Bact	7.075 ± 2.47, n=3	2.894 ± 0.7942, n=3	2.26 ± 0.4295, n=3	Control Vs Bacteria	0.0003
HPX8	-Bact	1.48 ± 0.9318, n=3	1.005 ± 0.1001, n=2	1.307 ± 0.6975, n=3	-	-
	+Bact	21.48 ± 8.114, n=3	23 ± 16.36, n=2	8.999 ± 3.119, n=3	Control Vs Bacteria	0.0002

Table S19 – HPX7 and HPX8 gene expression in the midgut after bacterial feeding. Related to Figure 4. Three independent experiments were performed and at least 2 biological replicates were used per condition. Each biological replicate is a pool of 10 mosquito midguts. Mann-Whitney U test. **All pools obtained were considered for statistical analysis.**

Gene	Treatment	Exp 1	Exp 2	Comparison	P value
HPX7	dsLacZ BF	1.024 ± 0.1581, n=3	1.018 ± 0.133, n=3	-	-
	dsIMPer BF	3.597 ± 1.062, n=3	7.038 ± 3.784, n=3	dsLacZ Vs dsIMPer	0.0022
HPX8	dsLacZ BF	1.233 ± 0.3213, n=5	0.7897 ± 0.2643, n=4	-	-
	dsIMPer BF	5.198 ± 2.485, n=5	34.09 ± 16.29, n=4	dsLacZ Vs dsIMPer	0.0040

Table S20 – HPX7 and HPX8 gene expression in the midgut in blood-fed *IMPer-silenced* mosquitoes. Related to Figure 4. Two independent experiments were performed, at least 3 biological replicates were used per condition. Each biological replicate is a pool of 10 mosquito midguts. Mann-Whitney U test. **All pools were considered for statistical analysis.**

Treatment	Exp 1	Exp 2	Exp 3	Comparison	P value
dsLacZ BF	25.33 ± 5.634, n=3	21.66 ± 9.546, n=3	34.29 ± 9.41, n=3	-	-
dsIMPer BF	47.67 ± 4.847, n=3	64.34 ± 14.45, n=3	60.86 ± 1.719, n=2	LacZ Vs IMPer	0.0003
dsHPX7 +BF	31.68 ± 2.978, n=3	34.08 ± 6.472, n=3	48.02 ± 2.13, n=2	LacZ Vs HPX7	0.3598
dsIMPer + dsHPX7 BF	21.16 ± 3.203, n=3	37.91 ± 10.08, n=3	35.95 ± 7.495, n=4	LacZ Vs IMPer + HPX7	0.7701

Table S21 – Effect of IMPer and HPX7 co-silencing on prostaglandin levels after blood feeding. Related to Figure 4. Three independent experiments were performed and at least 2 biological replicates were used per condition. Each biological replicate is a pool of 10 mosquitoes (hemolymph). *ANOVA* Dunn's multiple comparison test. **All pools were considered for statistical analysis.**

Treatment	Exp 1	Exp 2	Exp 3	Comparison	P value
dsLacZ BF	42.16 ± 6.438, n=6	39.21 ± 3.172, n=6	23.94 ± 2.45, n=8	-	-
dsIMPer BF	84.02 ± 17.09, n=6	44.96 ± 3.579, n=6	47.12 ± 5.179, n=4	LacZ Vs IMPer	0.0002
dsHPX8 BF	34.55 ± 2.85, n=6	29.47 ± 3.629, n=6	17.69 ± 2.705, n=4	LacZ Vs HPX8	0.6972
dsIMPer + dsHPX8 BF	36.5 ± 6.015, n=6	26.97 ± 3.242, n=6	24.6 ± 4.957, n=4	LacZ Vs IMPer + HPX8	0.8520

Table S22 - Effect of IMPer and HPX8 co-silencing on prostaglandin levels after blood feeding. Related to Figure 4. Three independent experiments were performed and at least 2 biological replicates were used per condition. Each biological replicate is a pool of 10 mosquitoes (hemolymph). ANOVA Dunn's multiple comparison test. **All pools were considered for statistical analysis.**

Treatment	Exp 1	Exp 2	Comparison	P value
dsLacZ BF	2, n=29	6, n=29	-	-
dsIMPer BF	5, n=28	14, n=29	LacZ Vs IMPer	0.0001
dsHPX8 BF	3, n=21	8, n=29	LacZ Vs HPX8	0.6805
dsIMPer + dsHPX8 BF	3, n=21	8, n=29	LacZ Vs IMPer + HPX8	0.1289

Table S23 – Effect of IMPer and HPX8 co-silencing on the number of hemocytes attached to midgut surface. Related to Figure 4. Two independent experiments were performed and at least 20 individual mosquitoes were analyzed per condition per experiment. Hemocyte numbers from the 2 experiments were combined for statistical analysis. *ANOVA* Kruskal-Wallis non-parametric test. **All individuals were considered for statistical analysis.**

Hemolymph injection from	Exp	Comparison	P value
dsLacZ BF	1.869 ± 0.3943, n=12	-	-
dsLacZ INF	6.148 ± 1.16, n=4	dsLacZ BF Vs dsLacZ INF	0.0022
dsHPX7 BF	3.189 ± 0.71, n=10	dsHPX7 BF Vs dsHPX7 INF	0.3930
dsHPX7 INF	2.365 ± 0.4351, n=10	-	-

Table S24 – Effect of HPX7 silencing on HDF production and granulocyte proportion after hemolymph transfer from mosquitoes control and *P.berghei* infected. Related to Figure 4. Granulocyte proportion from individual mosquitoes were used for statistical analysis. Mann-Whitney U test. **All individuals were considered for statistical analysis.**

Hemolymph injection from	Exp	Comparison	P value
dsLacZ BF	1.883 ± 0.2944, n=12	-	-
dsLacZ INF	6.069 ± 2.02, n=11	dsLacZ BF Vs dsLacZ INF	0.0036
dsHPX8 BF	2.63 ± 0.3749, n=14	dsHPX8 BF Vs dsHPX8 INF	0.5795
dsHPX8 INF	2.481 ± 0.5752, n=14	-	-

Table S25 – Effect of HPX8 silencing on HDF production and granulocyte proportion after hemolymph transfer from blood-fed control and *P.berghei* infected mosquitoes. Related to Figure 4. Granulocyte proportion from individual mosquitoes were used for statistical analysis. At least 11 individual mosquitoes were used per treatment. Mann-Whitney U test. **All individuals were considered for statistical analysis.**

Treatment	Exp 1	Exp 2	Comparison	P value
Hemolymph dsLacZ BF	114.5, n=14	71, n=21	LacZ BF Vs LacZ INF	0.0009
Hemolymph dsLacZ INF	39, n=17	19, n=30	LacZ BF Vs HPX8 BF	0.3876
Hemolymph dsHPX8 BF	111, n=15	41, n=21	HPX8 BF Vs HPX8 INF	0.5154
Hemolymph dsHPX8 INF	59.5, n=20	25, n=22	LacZ INF Vs HPX8 INF	0.0770

Table S26– Effect of HPX8 silencing on HDF production and antiplasmodial immunity after hemolymph transfer from blood-fed control and *P.berghei* infected mosquitoes. Related to Figure 4. Median number of oocysts per midgut 10 days post infection. Two independent infections were performed, and the number of parasites was counted in the midguts of individual mosquitoes. The 2 experiments were combined for statistical analysis. Mann-Whitney U test. **All mosquitoes were considered for statistical analysis. Table represents non-randomized data and therefore treatments have different numbers of individual mosquitoes. DsLacZ BF (total n=35); dsLacZ INF (total n=47); HPX8 BF (total n=36); HPX8 INF(total n=42).**

Accession Number	Gene	Primer sequence
AGAP004036	HPX7 qPCR Forward	GTTCTACAGTCCGCACACCA
	HPX7 qPCR Reverse	GCGTGGGATTGAGAAAGGTA
AGAP004038	HPX8 qPCR Forward	ATGGAGCGTTTTTGATCCAG
	HPX8 qPCR Reverse	TGATCCATCAGCGAGAAGAG
AGAP013327	IMPer qPCR Forward	GGGTGCTGTGTGACAATACG
	IMPer qPCR Reverse	CCATCGCGTTAAATTCACCT
AGAP009281	Evokin qPCR Forward	CAGCCGAAAGTGAACAAACA
	Evokin qPCR Reverse	ATGGTGGCCATTGTATACGG
AGAP010592	RpS7 qPCR Forward	AGAACCAGCAGACCACCATC
	RpS7 qPCR Reverse	GCTGCAAACTTCGGCTATTC

Table S27 – Oligonucleotides used for qPCR analysis. Related to Figures 3 and 4.

Transparent Methods

Mosquitoes, cell line and mouse feeding

Anopheles gambiae mosquitoes (G3 strain – CDC) were reared at 28^{o}C, 80% humidity under a 12h light/dark cycle and maintained with 10% Karo syrup solution during adult stages. Mosquito infections with *Plasmodium berghei* were performed using transgenic GFP *P.berghei* parasites (ANKA GFPcon 259cl2) maintained by serial passages into 3 to 4 week old female BALB/c mice (Charles River, Wilmington, MA, USA) from frozen stocks. Infectivity was measured by parasitemia levels and *in vitro* exflagellation counting as previously described (Billker et al., 1997). Four to five-day old mosquitoes were fed when mice reached 3-5% parasitemia and 1-2 exflagellation per field. Three to 4 weeks old uninfected mice were used to feed blood-fed control mosquitoes. After feeding, both control and infected mosquitoes were maintained at 19^{o}C, 80% humidity and 12h light/dark cycle until the day of hemolymph collection or dissection.

Ethics statement

Public Health Service Animal Welfare Assurance #A4149-01 guidelines were followed according to the National Institutes of Health Animal (NIH) Office of Animal Care and Use (OACU). These studies were done according to the NIH animal study protocol (ASP) approved by the NIH Animal Care and User Committee (ACUC), with approval ID ASP-LMVR5.

Prostaglandin sample preparation

Midguts and fat body were dissected in Hanks Buffer Salt Solution (HBSS) without calcium and magnesium and placed in a 24-well containing 400µl of HBSS with Calcium and Magnesium. Ten tissues were used for each biological replicate and were incubated for one hour at 28^{o}C for prostaglandin release. For total measurement of prostaglandins, the content of the well was homogenized with a pestle, frozen and thawed, and ultimately centrifuged at 12,000 rpm for 10

minutes at 4°C. The supernatant was stored at -80°C until assayed. To measure prostaglandin release by the midgut, ten midguts were placed in a 24-well plate and incubated for 1 hour at 28°C. Only the supernatant was collected and centrifuged before sample storage. For hemolymph samples, ten mosquitoes were perfused with 5µl each of HBSS with calcium and magnesium. Samples were centrifuged at 12,000 rpm for 10 minutes at 4^0C and stored at -80°C until assayed.

Prostaglandin ELISA assay

Hemolymph, midgut, and fat body prostaglandin levels were determined using Prostaglandin Screening ELISA and Prostaglandin E2 Monoclonal ELISA kit according to the manufacturer's instructions (Cayman Chemical, Ann Arbor, MI, USA). Briefly, 50 µl of standard/ sample was pipetted in a pre-coated 96-well plate. Aliquots (50 µl) of polyclonal PG antibody or monoclonal PGE2 antibody and PG or PGE2 conjugated to acetylcholinesterase (AChE) were added to each well and allowed to incubate at room temperature (PG screening kit) or 4°C (PGE2 monoclonal kit) for 18 hours. After incubation, wells were washed five times with 400 µl of wash buffer provided, followed by addition of 200 µl of Ellman's reagent substrate for development. Absorbance was read at 412nm with a Spectro fluorimeter plate reader (Molecular Devices, Sunnyvale, CA, USA) 90 minutes after addition of the substrate.

Hemocyte collection and quantification

Hemocytes were collected as previously described (Rodrigues et al., 2010, Ramirez et al., 2015). Briefly, a fine incision (half a millimeter) was made in the mosquito between the last 2 abdominal segments using fine-tip forceps, and then mosquitoes were injected into the thorax with an anticoagulant solution (60% Schneider's Insect medium, 10% fetal bovine serum, and 30% citrate buffer). Anticoagulant buffer was injected until 10 µl was recovered from the incision made in the abdomen using a sterile siliconized pipette tip. The collected sample was applied to a sterile

disposable haemocytometer slide (10 µl capacity, Neubauer Improved, iNCYTO C-Chip DHC-N01) and the hemocytes were counted under a light microscope (40x objective). Hemocytes were counted and the proportion of granulocytes was calculated relatively to the rest (prohemocytes and oenocytoids) for each individual mosquito.

Hemolymph collection and transfer

Hemolymph collection was performed as previously described (Rodrigues et al., 2010, Ramirez et al., 2015). In short, hemolymph was collected by perfusion as described above. Depending on the purpose of the experiment mosquitoes were perfused with either a modified anticoagulant buffer for transfer experiments (95% Schneider media, 5% citrate buffer) or HBSS with calcium and magnesium for ELISA assays. Each mosquito was injected with enough buffer to recover 5µl of hemolymph. Pools of ten mosquitoes were used for each biological replicate, for a total hemolymph volume of 50 µl. After collection, the hemolymph was centrifuged at 4^{o}C, 9,300g for 10 minutes to remove hemocytes. Cell-free hemolymph was then transferred to a new microcentrifuge tube and stored at -80^{o}C until used. Transfer of cell-free hemolymph to sugar fed naïve mosquitoes was done by microinjection of a total of 138nl per mosquito. We transferred the equivalent of one-fiftieth of the hemolymph from the donors to the recipients. The effect of cell-free hemolymph transfer was evaluated 4 days post injection by hemocyte counting in the recipients to determine granulocyte proportion.

Eicosanoid injection

3 to 4-day-old *An. gambiae* mosquitos were anesthetized on ice and injected with Prostaglandin E1, E2 or F2 (approximately 500 nM) (Cayman Chemical, Ann Arbor, MI, USA). Prostaglandin stock solutions were stored at -80^{o}C in 100% Ethanol. To perform mosquito injections, prostaglandins were dried under a stream of nitrogen gas and resuspended in modified

anticoagulant solution (95% Schneider media, 5% citrate buffer). Three days post-injection mosquitoes were either fed with a *P. berghei*-infected mouse to assess its effect on *Plasmodium* infection or perfused 4 days post injection to determine granulocyte proportion and collect hemolymph for further transfer.

Artificial feeding of bacteria from the microbiota

To isolate the mixture of bacteria used for feeding, sugar-fed mosquitoes from our colony were cleaned in 70% Ethanol and sterile PBS and dissected in sterile PBS. Pools of 5 midguts were placed in sterile PBS, homogenized and inoculated in liquid LB media to grow at 28^{o}C and 250rpm for at least 16 hours in a shaker incubator. The cultivable population was frozen and kept at -80^{o}C as stocks. A pre-inoculum was set up in LB media from the frozen stocks containing the bacterial mixture and allowed to grow overnight at 28^{o}C, 250rpm in a shaker incubator. On the day of the experiment, the pre-inoculum was diluted in fresh LB media and allowed to grow for 2 hours in the same condition described above. Briefly, after 2 hours of growth, bacteria were washed with sterile PBS to remove toxins and the concentration of the culture was estimated based on the Optical Density (OD) of the culture. At 600nm, 1OD was considered the equivalent of 10^9 bacteria/mL. 3 to 4-day-old mosquitos were treated with 10% sterile sucrose solution containing antibiotics Penicillin and Streptomycin (100U/mL and 100µg/mL, respectively) for 2 days prior the bacterial feeding. Control group was fed with a sterile 10% Bovine Serum Albumin (BSA) solution in HBSS without calcium and magnesium and the bacteria group was fed with the same solution containing 4 x 10^9 bacteria per feeder. Arachidonic acid 1µg/µl (Cayman Chemical, Ann Arbor, MI, USA) was supplemented in the 10% BSA solution to provide enough substrate for prostaglandin synthesis. Hemocyte biology and dynamics were analyzed 6 hours post feeding and prostaglandin production was evaluated 24 hours post feeding.

Visualizing hemocytes attached to the midgut basal lamina

To stain hemocytes, the day before any dsRNA treatment or feeding, 3 to 4-day-old mosquitoes were injected with 69nl of 100µM Vybrant CM-DiI cell labelling solution (ThermoFisher Scientific, Waltham, MA, USA) for a final concentration of approximately 3.5µM in the hemolymph. To preserve hemocyte-midgut attachment, tissues were quick fixed using a higher concentration of fixative injected straight into the hemolymph of the mosquito. Mosquitoes engorged from feeding either with 10% BSA solution or blood were ice-cold anesthetized, injected with 276nl of 16% paraformaldehyde, and rested for 40 seconds before midgut dissection in 4% paraformaldehyde solution. After dissection, midguts were placed in ice-cold PBS and opened longitudinally to remove the bolus. Cleaned, opened tissues were then fixed overnight at 4^{o}C in 4% paraformaldehyde. The following day, midguts were washed twice with PBS, blocked for 40 minutes with PBS containing 1% BSA, and washed twice with the same solution. For actin and nuclei staining, midguts were incubated for 30 minutes at room temperature with 1U of phalloidin (Alexa Fluor 647, Molecular Probes, ThermoFisher Scientific, Waltham, MA, USA) and 20µM Hoechst 33342 (405, Molecular Probes, ThermoFisher Scientific, Waltham, MA, USA), both diluted in PBS. Tissues were mounted in microscope slides using Prolong Gold Antifade Mountant (Molecular Probes, ThermoFisher Scientific, Waltham, MA, USA). Hemocytes were visualized by confocal microscopy and the number of hemocytes per midgut in each biological condition was also analyzed.

Midgut PGE2 Immunostaining

3 to 4-day-old mosquitoes were fed with 10% BSA solution with or without bacteria, as previously described. Six hours post feeding, mosquitoes were dissected in PBS, cleaned to remove bolus, and fixed using 4% paraformaldehyde overnight at 4^{o}C. Midguts were submitted to a mild

permeabilization with Tween 20 since prostaglandins are lipids and could be removed with this treatment. Then, midguts were blocked using PBS containing 1% BSA for 6 hours at room temperature and stained overnight using rabbit anti-PGE2 (1:300) (Anti-Prostaglandin E2 antibody, ab2318, Abcam, Cambridge, UK). Then midguts were washed with PBS containing 1% BSA and 0.1% gelatin and incubated with secondary antibodies goat anti-rabbit (Alexa Fluor 594, Molecular Probes, ThermoFisher Scientific, Waltham, MA, USA) (1:500) for 2 hours at room temperature. Midguts were washed three times with the same buffer, washed twice with PBS, and then incubated with 20µM Hoechst 33342 (405, Molecular Probes, ThermoFisher Scientific, Waltham, MA, USA) and 1U of phalloidin (Alexa Fluor 647, Molecular Probes, ThermoFisher Scientific, Waltham, MA, USA) as described above. Microscope slides were mounted using Prolong Gold Antifade Mountant (Molecular Probes, ThermoFisher Scientific, Waltham, MA, USA).

Agarose-spot migration assay

A protocol was adapted from Wiggins & Rappoport, 2010 (Wiggins and Rappoport, 2010). Briefly, 1% low melting agarose solution in PBS was heated on a hot plate to facilitate the dissolution of the agarose. After complete dissolution, 1% low melting agarose solution was placed at 40^{o}C to cool down. For the prostaglandins, the equivalent of 7.1 µg was dried under a nitrogen gas stream in a glass tube to remove the ethanol and resuspended in 5µl of sterile PBS. Five microliters of the cooled down 1% low melting agarose solution was mixed with 5µl of PBS with or without prostaglandins. A ten-microliter drop was placed in a 35mm glass-bottom dishes (Mat Tek corporation, Ashland, MA, USA). The chamber was then placed at 4^{o}C for 5 minutes and the media containing 5 x 10^{5} Sua 5.1 cells was pipetted in the well. Four hours after seeding the cells, the complete media was replaced by Schneider media 1% FBS and analyzed next morning by

counting the number of cells that entered the agarose per field. Imaging was performed on a Leica Epifluorescence (Leica Microsystems, Wetzlar, Germany) inverted microscope with a 40x objective using phase contrast and migration was recorded overnight every minute.

Hemocyte Live Imaging

3 to 4 days old mosquitoes were treated with sterile sucrose 10% solution containing antibiotics as described above. The next day mosquitoes were fed with saline solution with sodium bicarbonate (0.15M NaCl and 0.01M Na_2CO_3, pH 7.4) containing CFDA-SE (Molecular Probes, ThermoFisher Scientific, Waltham, MA, USA) 1:500 for midgut staining to use as a reference. Then, only engorged mosquitoes were injected with a lipophilic dye, Vybrant DiD cell-labelling solution (Abs 644/ Em 665, Molecular probes, ThermoFisher Scientific, Waltham, MA, USA), for hemocyte identification and starved until the next day. Mosquitoes were fed with 10% BSA solution with or without bacteria as described above. After 4 hours post feeding, mosquitos were imaged between a coverslip and glass slide at 1-minute intervals using variable z-steps. To quantify hemocyte behavior, images from 2 hours of acquisition were analyzed using Imaris 8.3.1 (Bitplane, Concord, MA, USA). Hemocytes were first automatically identified and tracked. Next, tracks were manually edited and corrected for sample drift. Visualization of tracks was graphed using the Imaris MATLAB XTension "Plot all tracks with a common origin" (Peter Beemiller). Track statistics were exported and analyzed in Prism (GraphPad, San Diego, CA, USA) using the Mann-Whitney test with outliers removed.

Confocal Microscopy

Images were captured using a Leica TCS SP5 confocal microscope (Leica Microsystems, Wetzlar, Germany) with a 63x oil immersion objective (zoom factor of 4) equipped with a photomultiplier tube/hybrid detector. Samples were visualized with a 488-nm argon laser for CFDA-SE (midgut

staining for live imaging), a DPSS 561-nm laser for CM-DiI, a HeNe 594-nm laser for Alexa Fluor 594 (rabbit secondary antibody), and a HeNe 633-nm laser for Alexa Fluor 633 (phalloidin). Hoechst was excited using a 405-nm diode laser. Images were taken using sequential acquisition and variable z-steps. Image processing was performed using Imaris 8.3.1 (Bitplane, Concord, MA, USA) and Adobe Photoshop CC (Adobe Systems, San Jose, CA, USA).

dsRNA synthesis

The RNA interference (RNAi) silencing of heme-peroxidases (HPX7, HPX8 and IMPer) and Evokin was performed as previously described (Oliveira Gde et al., 2012, Ramirez et al., 2015, Kumar et al., 2010). In short, 3 to 4-day-old female *An. gambiae* were cold-anesthetized and injected with 69nl of a 3-µg/µl dsRNA solution specific for each gene. DsRNA was generated from a cDNA template from *A.gambiae* and the MEGAscript RNAi kit (ThermoFisher Scientific, Waltham, MA, USA). Primers were designed specifically for targeted genes and are listed as follows: for HPX7 (AGAP004036), a 689 bp fragment was amplified with external primers (F-AACTGTCCTCCACGCTGTTT and R- CACCCTGGGCAAGTATTCAC), the product of this reaction was amplified again using internal primers containing T7 promoters and generating a smaller fragment, 418 bp (F-TAATACGACTCACTATAGGGATCAAAACGAAGGCCAAATG and R-TAATACGACTCACTATAGGGCCAGCGAGATCAACTGGTTC). For HPX8 (AGAP004038), the same strategy was used, where a 718 fragment was amplified using external primers (F- AACCACCAACGCTATCGAAC and R- CGACATAAACTGGCCGAACT). Using the external PCR product as template a smaller fragment (450 bp) was amplified with T7 promoters (F- TAATACGACTCACTATAGGGTCACTGCCGTTTGAACTGTC and R-TAATACGACTCACTATAGGGCCACACACCGTCCTCGTAG). For IMPer (AGAP013327), a

463-bp fragment was amplified containing T7 promoters straight from cDNA (F-TAATACGACTCACTATAGGGTCGGTGCTGGAAAAGGATGG and R-TAATACGACTCACTATAGGGGTTGGCGCGAGCTAAACACG). For Evokin (AGAP009281), a 166-bp fragment was amplified with T7 promoters from cDNA (F-TAATACGACTCACTATAGGGTGGCGGTACTCCTGCTACTC and R-TAATACGACTCACTATAGGGGCCGTTATACACTTCCCACC). A 218-bp fragment was amplified from LacZ gene cloned into pCRII-TOPO vector using M13 primers to generate a dsRNA control as previously described (Molina-Cruz et al., 2012). Gene silencing efficiency obtained with this method was 81% for HPX7, 60% for HPX8, 97% for IMPer in the midgut and 80% for Evokin in the fat body.

RNA extraction, cDNA synthesis, and qPCR analysis

RNA samples from midguts were obtained using TRIzol (ThermoFisher Scientific, Waltham, MA, USA) according to manufacturer instructions. Briefly, pools of 15 midguts were dissected in PBS, placed in TRIzol, and homogenized with a motorized pestle. Two hundred microliters of chloroform were added (1/5 of TRIzol volume) to 1mL of TRIzol for the aqueous phase separation. Total RNA was precipitated with 2-propanol (1:1) added to the aqueous phase and resuspended in 30µl of nuclease free water. RNA concentration was measured at 260nm using a Nanodrop (ThermoFisher Scientific, Waltham, MA, USA). One microgram of total RNA was used for complementary DNA (cDNA) synthesis using Quantitect Reverse Transcription Kit (Qiagen, Hilden, Germany) according to manufacturer's instructions. Gene expression was assessed by quantitative PCR (qPCR) using the resulting cDNA as a template. We used the DyNamo SYBR green qPCR kit (ThermoFisher Scientific, Waltham, MA, USA) with target specific primers listed on table S27 and the assay ran on a CFX96 Real-Time PCR Detection System (Bio-Rad, Hercules,

CA, USA). Relative quantitation results were normalized against *An. gambiae* ribosomal protein S7 (RpS7) as internal standard and analyzed using the ΔΔCt method (Livak and Schmittgen, 2001, Pfaffl, 2001). Statistical differences of fold change values between the conditions was determined using the Mann-Whitney test (GraphPad, San Diego, CA, USA). Each independent experiment was done with three biological replicates (three pools of 15 tissues) for each condition tested, and each one was analyzed by qPCR in duplicates (technical replicates). At least three independent experiments were performed.

Statistical analysis

All statistical analyses were performed using GraphPad Prism 5 (GraphPad, San Diego, CA, USA). All analyses where pertinent were conducted using either the student Unpaired t-test, Mann-Whitney Test, ANOVA Dunnett multiple comparison and ANOVA Kruskal-Wallis test. The test choice was determined based on the variation of the sample, if parametric or non-parametric, and the number of treatments in each experiment. Significance was assessed at $p < 0.05$. The error bars represent the Standard Error of the Mean (SEM).

Key resources table

REAGENT or RESOURCE	SOURCE	IDENTIFIER
Antibodies		
Rabbit Polyclonal anti-PGE2	Abcam	Ab2318
Anti-Rabbit IgG Alexa Fluor 594	Molecular Probes/ Invitrogen/ ThermoFisher Scientific	A-11037
Cell lines		
Anopheles gambiae Sua 5.1*	BEI Resources	MRA-922
Organisms strains		
Anopheles gambiae G3 strain (CDC)	BEI Resources	MRA-112
GFP - *Plasmodium berghei* (ANKA GFPcon 259cl2)	BEI resources	MRA-865
BALB/c mice	Charles River	N/A
Chemicals		

Hanks Buffer Salt Solution (HBSS) with Calcium and Magnesium	Sigma	H8264
Hanks Buffer Salt Solution (HBSS) without Calcium and Magnesium	Sigma	H6648
Prostaglandin Screening ELISA kit	Cayman Chemical	514012
Prostaglandin E2 Monoclonal ELISA kit	Cayman Chemical	514010
Schneider's Insect Medium	Sigma	S0146
Prostaglandin E2	Cayman Chemical	14010
Prostaglandin F2α	Cayman Chemical	16010
Prostaglandin E1	Cayman Chemical	13010
Bovine serum albumin, fatty acid free	Sigma/ Roche	10775835001
Penicillin-Streptomycin	Sigma	P4333
Arachidonic Acid	Cayman Chemical	90010
Vybrant CM-DiI cell labeling solution	Molecular Probes/ Invitrogen/ ThermoFisher Scientific	V22888
Alexa Fluor 647 Phalloidin	Molecular Probes/ Invitrogen/ ThermoFisher Scientific	A22287
Hoechst 33342 solution (20 mM)	Molecular Probes/ Invitrogen/ ThermoFisher Scientific	62249
Prolong Gold Antifade Mountant	Molecular Probes/ Invitrogen/ ThermoFisher Scientific	P36934
16% Paraformaldehyde	Electron Microscopy Sciences	15710
Vybrant CFDA-SE	Molecular Probes/ Invitrogen/ ThermoFisher Scientific	V12883
Vybrant DiD cell labelling solution	Molecular Probes/ Invitrogen/ ThermoFisher Scientific	V22887
MEGAscript RNAi kit	ThermoFisher Scientific/ Invitrogen	AM1626
TRIzol reagent	ThermoFisher Scientific/ Invitrogen	15596018
QuantiTect Reverse Transcription Kit	Qiagen	205314
DyNAmo HS SYBR Green qPCR Kit	ThermoFisher Scientific	F410L
Oligonucleotides		
Primers for cloning, dsRNA synthesis and qPCR	This paper/ Eurofins	N/A
Software		
Graphpad Prism	GraphPad	N/A

IMARIS 8.3.1	Bitplane	N/A
Adobe Photoshop CC	Adobe Systems	N/A
Specific Tools used in this manuscript		
SKC, Inc. C-Chip™ Disposable Hemacytometers (Neubauer Improved)	Fisher Scientific	SKC, Inc. DHCN015
35mm Dish/ High tolerance 1.5 Coverslip/ 14mm Glass Diameter	Mat Tek corporation	P35G-0.170-14-C

Supplemental References

BILLKER, O., SHAW, M. K., MARGOS, G. & SINDEN, R. E. 1997. The roles of temperature, pH and mosquito factors as triggers of male and female gametogenesis of Plasmodium berghei in vitro. Parasitology, 115 (Pt 1), 1-7.

RODRIGUES, J., BRAYNER, F. A., ALVES, L. C., DIXIT, R. & BARILLAS-MURY, C. 2010. Hemocyte differentiation mediates innate immune memory in Anopheles gambiae mosquitoes. Science, 329, 1353-5.

RAMIREZ, J. L., DE ALMEIDA OLIVEIRA, G., CALVO, E., DALLI, J., COLAS, R. A., SERHAN, C. N., RIBEIRO, J. M. & BARILLAS-MURY, C. 2015. A mosquito lipoxin/lipocalin complex mediates innate immune priming in Anopheles gambiae. Nat Commun, 6, 7403.

WIGGINS, H. & RAPPOPORT, J. 2010. An agarose spot assay for chemotactic invasion. Biotechniques, 48, 121-4.

OLIVEIRA GDE, A., LIEBERMAN, J. & BARILLAS-MURY, C. 2012. Epithelial nitration by a peroxidase/NOX5 system mediates mosquito antiplasmodial immunity. Science, 335, 856-9.

KUMAR, S., MOLINA-CRUZ, A., GUPTA, L., RODRIGUES, J. & BARILLAS-MURY, C. 2010. A peroxidase/dual oxidase system modulates midgut epithelial immunity in Anopheles gambiae. Science, 327, 1644-8.

MOLINA-CRUZ, A., DEJONG, R. J., ORTEGA, C., HAILE, A., ABBAN, E., RODRIGUES, J., JARAMILLO-GUTIERREZ, G. & BARILLAS-MURY, C. 2012. Some strains of Plasmodium falciparum, a human malaria parasite, evade the complement-like system of Anopheles gambiae mosquitoes. Proc Natl Acad Sci U S A, 109, E1957-62.

LIVAK, K. J. & SCHMITTGEN, T. D. 2001. Analysis of relative gene expression data using real-time quantitative PCR and the 2(-Delta Delta C(T)) Method. Methods, 25, 402-8.

PFAFFL, M. W. 2001. A new mathematical model for relative quantification in real-time RT-PCR. Nucleic Acids Res, 29, e45.